Catalysis Letters 2 (1989) 351–360

TPD/TPR AND QUANTUM CHEMICAL STUDY OF METHANOL INTERACTION WITH $H_{3+n}PV_nMo_{12-n}O_{40}$ HETEROPOLYACIDS

E.M. SERWICKA, E. BROCLAWIK, K. BRUCKMAN and J. HABER

Institute of Catalysis and Surface Chemistry, Polish Academy of Sciences, 30-239 Krakow, ul. Niezapominajek I, Poland

Received 21 January 1989; revised 13 April 1989

Quantum chemical calculations of the electronic structure, charge distribution, bond lengths and angles have been carried out for different species involved in the transformation of methanol along acid-base and redox reaction pathways. Results are compared with the TPD/TPR measurements of methanol interaction with $H_{3+n}PV_nMo_{12-n}O_{40}$ heteropolyacids.

1. Introduction

Most of the attempts to use heteropolycompounds as catalysts have been devoted to those containing the best characterized anion known as the Keggin unit (fig. 1). Particular attraction of these compounds lies in the versatility of their composition which allows one to design the acidic and redox properties by a suitable choice of the constituent elements [1]. On the other hand, the Keggin unit provides a microsurface of known structure and as such is particularly suitable for mechanistic studies [1,2].

Conversion of methanol over heteropolycompounds is known to give various products depending on the catalyst composition, i.e. its acidic and oxidizing

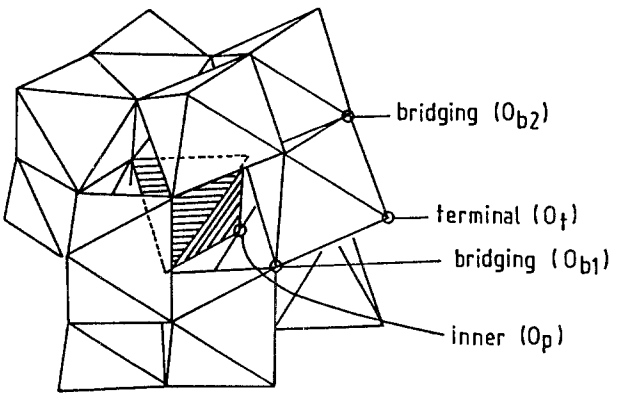

Fig. 1. Structure of the Keggin anion.

functions [3–6]. It has been found, for instance, that strongly acidic catalysts based on 12-tungstophosphoric anion are active in hydrocarbon production via dimethylether intermediate [3–5]. On the other hand, Sorensen and Weber [6] demonstrated that gradual substitution of tungsten with vanadium enhances oxidizing ability of the Keggin anion and as a result, increasing amounts of formaldehyde, the product of oxidative dehydrogenation, appear on the expense of the dimethylether yield.

A mechanistic scheme has been proposed [7,8] in which formation of surface methoxy groups, documented by IR and ^{13}C MAS NMR experiments, was postulated as the result of methanol interaction with surface hydroxyl groups of acidic character. Such methoxy groups may further react to form dimethylether, or undergo dehydrogenation to give formaldehyde.

A fundamental question arises at this point as to which molecular interactions operating at the surface of the catalyst are responsible for the transformation of methoxy species along either of the two possible reaction pathways. It seemed therefore of interest to examine with quantum chemical methods the electronic structure of different species involved in these processes and to substantiate the proposed mechanism with the possible HOMO-LUMO interactions. In order to correlate the reaction pattern with the properties of the catalyst, TPD/TPR technique with mass spectroscopic detection of desorption/reaction products was used to follow the product distribution of methanol interaction with the $H_{3+n}PV_nMo_{12-n}O_{40}$ heteropolyacids. This series of solids has been chosen because from the solution studies it is known that substitution with vanadium affects both the redox and the acid-base properties of 12-molybdophosphate anion, increasing its oxidizing power and lowering acidity [1,9]. Thus, it could be expected that the solid catalysts would, partially at least, reflect these trends, and influence accordingly the product distribution in methanol conversion.

2. Experimental

2.1. MATERIALS

The $H_{3+n}PV_nMo_{12-n}O_{40} \cdot xH_2O$ ($n = 0, 1, 2, 3$) heteropolyacids were prepared according to the method of Tsigdinos and Hallada [10]. They are further abbreviated H_3, H_4, H_5 and H_6. Prior to the TPD experiments samples were calcined at 623 K for 3 hours in order to ensure the TPD data to be free of phenomena accompanying thermal dehydration/decomposition of the acids. The BET surface area of the calcined samples was 1–3 m^2/g.

2.2. TEMPERATURE PROGRAMMED DESORPTION/REACTION

In the TPD/TPR experiments with methanol the sample of 60 mg was first outgassed at 573 K for 0.5 h at the pressure of 5×10^{-3} Torr. Then 20 μl of

methanol were introduced at 293 K and the adsorption carried out for 0.5 h. The sample was then outgassed at 373 K for 1 h and the TPR experiment was carried out in the temperature range 373–723 K at the heating rate 10 K/min. Desorbing products were analysed with a mass spectrometer. The TPR profile of formaldehyde was generated by plotting the *m/e* 30 value after correction for the methanol and methyl formate fragmentations; *m/e* 32 after correction for methyl formate fragmentation was used to monitor methanol, and *m/e* 45 to follow the changes of dimethylether concentration. TPD of pyridine was performed with 100 mg samples according to a similar procedure [11]. Predesorption of pyridine was carried out at 423 K and the TPD run in the temperature range 423–723 K. Desorption profile was generated by monitoring the *m/e* 79 changes. Mass spectral intensities have not been adjusted according to sensitivity differences and therefore do not represent absolute partial pressures.

2.3. QUANTUM CHEMICAL CALCULATIONS

A semiempirical MNDO method [12] with automatic geometry optimization was used to investigate the electronic structure, charge distribution, bond lengths and angles of methanol and related intermediates.

3. Results and discussion

We use the reaction framework proposed by Highfield and Moffat [8] and extended by Farneth et al. [7] to identify the intermediate compounds for the quantum chemical calculations.

$$CH_3OH + H^+ \ldots O_{KU} \rightarrow CH_3OH_2^+ \ldots O_{KU} \quad (1)$$

$$CH_3OH_2^+ \ldots O_{KU} \rightarrow CH_3^+ \ldots O_{KU} + H_2O \quad (2)$$

$$CH_3^+ \ldots O_{KU} + CH_3OH \rightarrow CH_3OCH_3 + H^+ \ldots O_{KU} \quad (3)$$

$$CH_3^+ \ldots O_{KU} + O_{KU} \rightarrow CH_2O + H^+ \ldots O_{KU} \quad (4)$$

where O_{KU} represents an O^{2-} ion of the Keggin unit, H^+ is a Broensted acid site, $CH_3OH_2^+ \ldots O_{KU}$ a protonated methanol/Keggin anion pair, and $CH_3^+ \ldots O_{KU}$ is effectively a methoxy group CH_3O^- built into the Keggin structure.

Our MNDO calculations give following HOMO and LUMO for the organic species involved (y-axis = molecule axis):

(*a*) *methanol molecule* CH_3OH

$\Psi_{HOMO} = -0.83\ p_x(O) + 0.28\ p_x(C) - 0.34\ s(H^2_{CH}) + 0.34\ s(H^3_{CH})$

$\Psi_{LUMO} = -0.68\ p_z(C) + 0.52\ s(H^1_{CH}) - 0.26\ s(H^2_{CH}) - 0.26\ s(H^3_{CH}) - 0.29\ s(H_{OH})$.

HOMO represents a bonding orbital localized mainly on the oxygen atom, while LUMO is the first orbital of the antibonding system, associated mainly with the

CH_3 group. The calculated C–O bond length is 1.39 Å, the carbon atom carries positive charge of 0.19 *e*.

(*b*) *protonated methanol molecule* $CH_3OH_2^+$

$\Psi_{HOMO} = 0.53\ p_z(O) - 0.57\ p_z(C) - 0.52\ s(H^1_{CH}) + 0.26\ s(H^2_{CH}) + 0.26\ s(H^3_{CH})$

$\Psi_{LUMO} = 0.41\ s(O) - 0.21\ s(C) + 0.61\ p_y(C) - 0.44\ s(H^1_{OH}) - 0.44\ s(H^2_{OH})$.

Here, HOMO's highest electron density is associated with the CH_3 group, while LUMO has comparable contributions from all but methyl structural elements. The C–O bond becomes elongated to 1.46 Å and the carbon atom increases its positive charge to 0.23 *e*, as intuitively predicted by Moffat et al. [13].

(*c*) *methoxy group* CH_3O^-

Both HOMO and LUMO are doubly degenerated.

$\Psi^1_{HOMO} = 0.43\ p_x(O) - 0.73\ p_z(O) + 0.37\ s(H^1_{CH}) - 0.37\ s(H^3_{CH})$

$\Psi^2_{HOMO} = -0.73\ p_x(O) - 0.43\ p_z(O) + 0.21\ s(H^1_{CH}) - 0.43\ s(H^2_{CH}) + 0.21\ s(H^3_{CH})$

$\Psi^1_{LUMO} = 0.24\ p_x(O) - 0.68\ p_x(C) - 0.39\ p_z(C) + 0.23\ s(H^1_{CH}) - 0.46\ s(H^2_{CH}) + 0.23\ s(H^3_{CH})$

$\Psi^2_{LUMO} = -0.24\ p_z(O) - 0.39\ p_x(C) + 0.68\ p_z(C) - 0.39\ s(H^1_{CH}) + 0.39\ s(H^3_{CH})$.

HOMOs carry the highest electron density at the oxygen atom, while LUMOs are localized predominantly on the CH_3 group and are antibonding with respect to the C–H and C–O bonds.

According to recent detailed calculations by Taketa et al. [13] HOMO of the $(PMo_{12}O_{40})^{3-}$ anion is in 94% composed of the 2p lone pir orbitals of the bridging oxygens O_b. The LUMO is a mixture of the Mo 4d orbitals (50%) and the O_b 2p orbitals (48%) and is antibonding with respect to the Mo–O_b bond.

After taking into account all conceivable HOMO-LUMO interactions, the molecular mechanism of methanol interaction with the Keggin anion, shown in fig. 2, may be envisaged.

Its first step represents an electrophilic attack of the acidic proton associated with the Keggin unit on methanolic oxygen whose orbital 2p contributes in ca. 70% to the HOMO of methanol (configuration I). As a result, an intermediate complex corresponding to a protonated methanol molecule $CH_3OH_2^+$ with substantially elongated C–O bond and carbon atom bearing an increased positive charge is formed (configuration II). Subsequent nucleophilic attack of a lone pair of neighbouring bridging oxygen (Keggin's HOMO) is directed towards the carbon of the $CH_3OH_2^+$ complex where LUMO has the largest coefficient. This results in the C–O bond cleavage to give a methoxy group occupying a bridging site, and a molecule of water (configuration III).

Production of formaldehyde from the methoxy group, (eq. (4)), requires a proton abstraction and a reduction of the catalyst by two electrons. In terms of HOMO-LUMO interactions we propose the first step to be an attack of the Keggin bridging oxygen lone pair on the methoxy group LUMO localized predominantly on the CH_3 group. In view of the antibonding character of the latter, this will weaken the C–H bond and enable an effective proton capturing

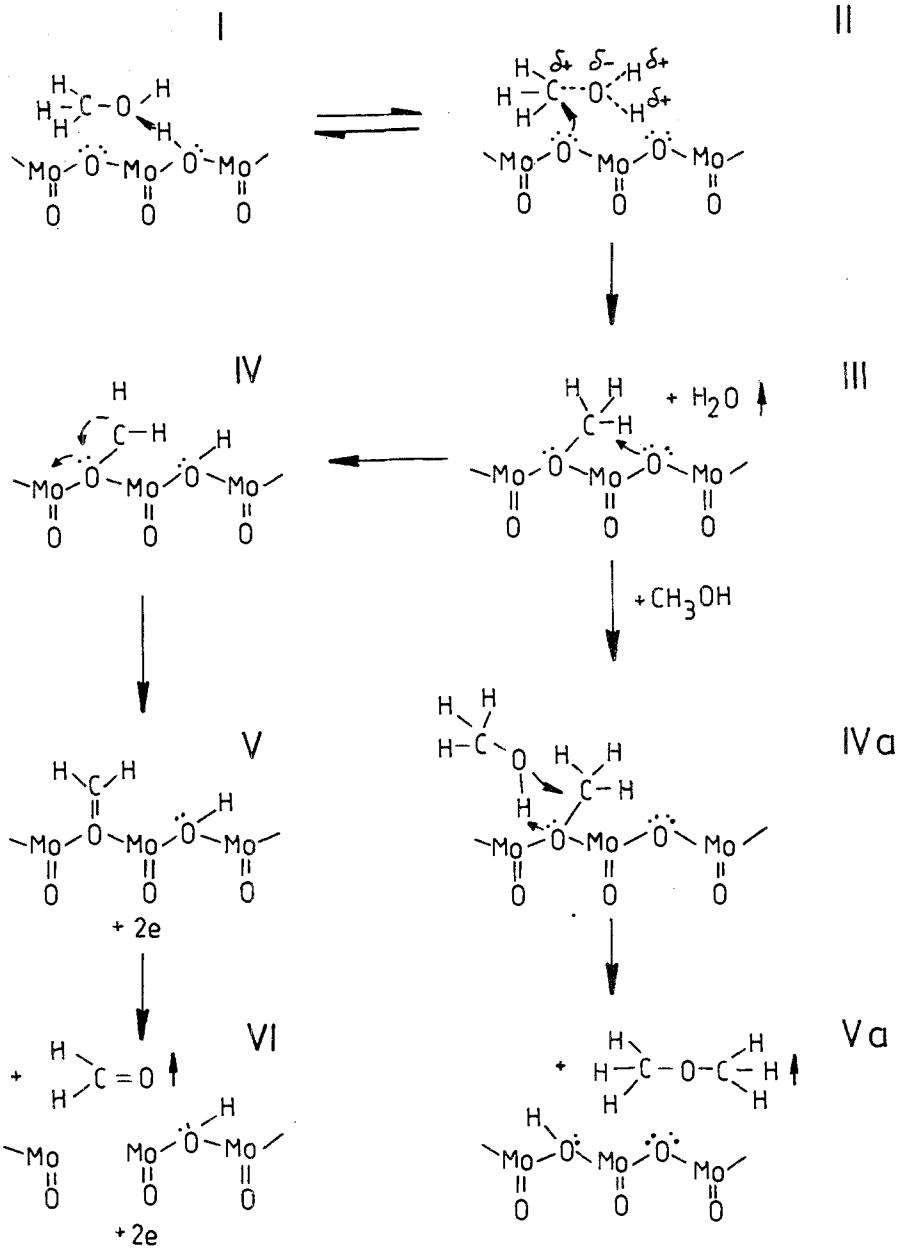

Fig. 2. Mechanism of methanol interaction with the Keggin anion.

by O_b leading to the configuration IV. The latter will rapidly reform to give configuration V which involves the transfer of two electrons to the catalyst via the carbon-oxygen π-system and is equivalent with the reduction of the solid. Configuration V represents effectively a formaldehyde molecule coordinated to the Keggin unit at the bridging site. The reduction electrons introduced into the

heteropolyanion occupy its LUMO which is antibonding with respect to the $Mo-O_b$ bond. This leads to weakening of this bond and facilitates its dissociation and desorption of the CH_2O molecule.

According to eq. (3) dimethylether is formed in a competitive reaction between the methoxy group (intermediate III) and a methanol molecule. This process requires a C–O bond scission in one of the reactants. We suggest that it is the C–O bond of the methoxy group that breaks to give dimethylether because there is an antibonding contribution with respect to the C–O bond in the LUMO of methoxy group, while the LUMO of methanol bears no such a character. Indeed, our quantum chemical calculations [14] show that when a methanol molecule approaches methoxy group attached to a metal centre the methoxy C–O bond breaks. The sp^3 hybrydization of bridging oxygens results in an outward orientation of both the methyl group and the lone pair making the latter capable of interaction with approaching methanol molecule. Therefore one at least of the possible pathways of dimethylether formation may proceed via a concerted nucleophilic attack of methoxy oxygen on the methanol hydrogen and of methanolic oxygen on the methoxy carbon, as shown in configurations IVa and Va. The other conceivable source of dimethylether could stem from the reaction involving two neighbouring methoxy groups and would effectively remove one of the bridging oxygens of the Keggin.

Major species appearing on TPD/TPR of methanol from all investigated samples are methanol itself, water, dimethylether, formaldehyde, and carbon monoxide, in agreement with previous findings for the $K_{3-x}H_xPMo_{12}O_{40}$ material [7]. Small amounts of methyl formate are also produced. We shall concentrate our attention on the unreacted methanol, dimethylether and formaldehyde yields, since they are most significant for the chemistry of the methanol-heteropolyacid systems. Figure 3 shows the TPD profiles, figure 4 yields of the respective species. It may be seen that substitution with vanadium enhances the evolution of all species in question. There is also an increasing contribution from the low temperature desorption peak on the TPD profile of formaldehyde. Changes in the TPD profile of dimethylether involve an increasing contribution from the high temperature desorption.

TPD of pyridine from the calcined acids [11] shows that gradual substitution with vanadium lowers the acidity of the series (fig. 5). Parallel IR measurements have proved that the acidity is predominantly of Broensted type [10]. Pyridine desorbs from the investigated samples in a number of overlapping TPD peaks, indicating the presence of centres of different acid strength. The overall trend of a decreasing acidity as the number of vanadium atoms increases is accompanied by a shift towards relatively weaker acid sites. The insert in fig. 5 shows the desorption profile from the H_6 sample calcined at temperature by 150 K lower than the standard treatment. It clearly shows that the occurrence of strongest acid sites is associated with the amount of water retained by the bulk of the acid phase. This is in agreement with earlier findings pointing out that the proton

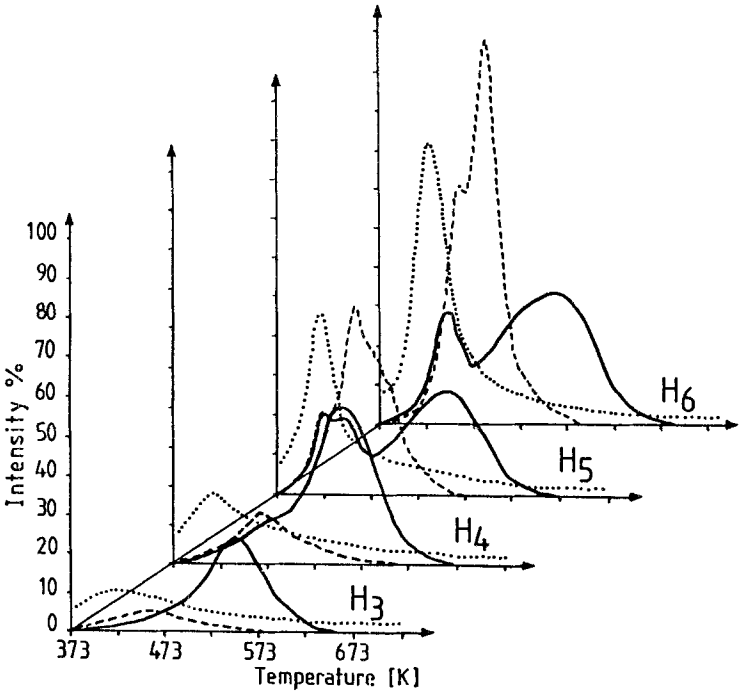

Fig. 3. TPD/TPR of methanol from the $H_{3+n}PV_nMo_{12-n}O_{40}$ samples. ——— formaldehyde, - - - - - - dimethylether, ····· methanol.

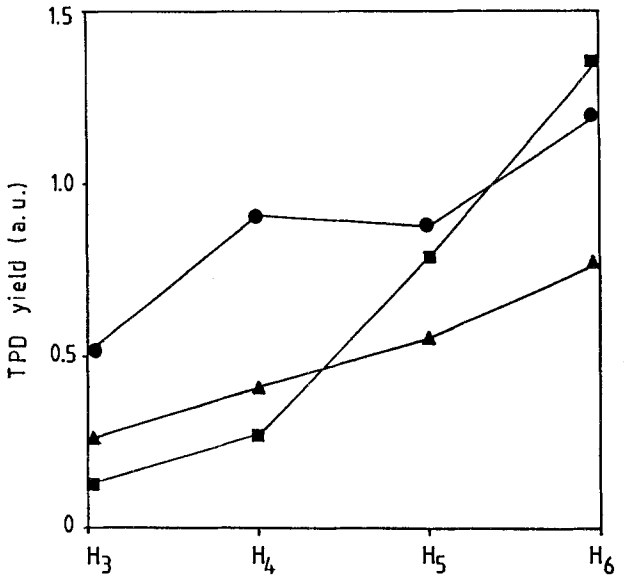

Fig. 4. TPD yield of formaldehyde (●), dimethylether (■), and methanol (▲) from the $H_{3+n}PV_nMo_{12-n}O_{40}$ samples.

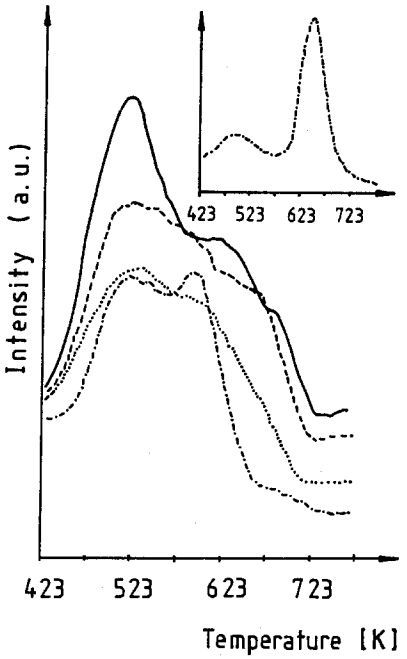

Fig. 5. TPD of pyridine from the $H_{3+n}PV_n\ Mo_{12-n}O_{40}$ samples. ——— H_3, ------ H_4, ····· H_5, ·—·—· H_6.

mobility in the heteropolyacid secondary structure increases with its hydration degree [1].

The observed decreasing trend in the number of acid sites as substitution with vanadium proceeds may look puzzling in view of the simultaneous increase of the Keggin anion charge, and, as a result, of the total number of constitutional protons available. This means that the amount of the acid centres strong enough to be seen by pyridine after outgassing of weakly adsorbed species at 423 K represents only a fraction of the constitutional protons present in each sample and decreases on gradual substitution with vanadium. According to TPD strongly adsorbed pyridine detects only 12% (H_3), 8% (H_4), 6% (H_5), and 5% (H_6) of the constitutional protons. This signifies that the majority of protons present in these samples constitute relatively weak acid centres, rather firmly bound to the Keggin anion, their amount increasing with number of vanadium atoms.

Substitution with vanadium results in changes of the charge distribution within the Keggin anion. In particular, from the ^{17}O NMR data reported by Maksimovskaya et al. [15], it is known that the electron density on the bridging oxygens of the Mo-O-Mo type systematically increases. This implies a greater driving force for a nucleophilic attack on the C–H bond of the methoxy group shown in configuration II and therefore should enhance the reaction path leading to formaldehyde. Simultaneously, higher proton affinity of bridging oxygens and higher oxidation potential of vanadium would facilitate proton abstraction and

electron transfer to the Keggin anion and thus promote formaldehyde desorption. Indeed, a rise in the CH_2O evolution on gradual replacing of Mo by V is observed (fig. 4), accompanied by the appearance of additional peaks on the low temperature side of main desorption, as expected for the surface containing sites of different proton and electron affinities.

Evolution of dimethylether also increases with vanadium content and so does that of unreacted methanol. This signifies that the total amount of methanol which remains in the catalysts after outgassing at 373 K increases with vanadium substitution, i.e. with increasing total number of Broensted acidic sites. It seems therefore that proton affinity of methanol is high enough to enable protonation even by the relatively weak acid centres present in the calcined acids. On the other hand, from the acidity measurements it follows that the amount of strong acid sites decreases within the series. This means that under TPD conditions an increasing amount of methanol will desorb due to the shift from configuration II to I before having a chance to transform from configuration II to III. Increasing amounts of evolving methanol promote in turn the transformation of methoxy groups along the dehydration pathway, i.e. following configurations IVa and Va, to give dimethylether. An increasing contribution from the high temperature TPR peak of dimethylether indicates that in this temperature range another mechanism of dimethylether production, possibly involving reaction of two neighbouring methoxy groups with an effective elimination of one of the bridging oxygens, may operate as well.

4. Conclusions

Mechanism of methanol interaction with $H_{3+n}PV_nMo_{12-n}$ ($n = 0, 1, 2, 3$) heteropolyacids proposed on the basis of the TPD/TPR experiments and quantum chemical calculations shows that both the dimethylether (product of dehydration), and the formaldehyde (result of oxidative dehydrogenation), are produced from the same methoxy intermediate. Substitution with vanadium enhances nucleophilic properties of Keggin bridging oxygens and promotes transformation into formaldehyde. Increasing with vanadium content amounts of unreacted methanol enhance in turn the dehydration pathway.

Acknowledgements

E.M.S. gratefully acknowledges the grant from the Austrian Academy of Sciences and would like to thank Professor J. Lercher from the Institute of Physical Chemistry of Technical University Vienna for the possibility to use the TPD equipment in his laboratory and for many valuable discussions.

References

[1] M. Misono, Catal. Rev.-Sci. Eng. 29 (1987) 269, and the references therein.
[2] E.M. Serwicka, J.B. Black and J.B. Goodenough, J. Catal. 106 (1987) 23.
[3] J.B. Monagle and J.B. Moffat, J. Catal. 91 (1985) 132 and the references therein.
[4] Y. Ono, T. Mori and T. Keii, in: *Proc. 7th Int. Congress in Catalysis, Tokyo, 1980* (Kodansha, Tokyo, 1980) 1414.
[5] T. Baba, J. Sakai, H. Watanabe and Y. Ono, Bull. Chem. Soc. Jpn. 55 (1982) 2555.
[6] C.M. Sorensen and R.S. Weber, in: *Proc. 2nd China-U.S.-Japan Seminar on Heterogeneous Catalysis, Berkeley, 1985.*
[7] W.E. Farneth, R.H. Staley, P.J. Domaille and R.D. Farlee, J. Am. Chem. Soc. 109 (1987) 4018.
[8] J.G. Highfield and J.B. Moffat, J. Catal. 95 (1985) 108.
[9] I.V. Kozhevnikov, Khimiya 12 (1985) 1.
[10] G.A. Tsigdinos and C.J. Hallada, Inorg. Chem. 7 (1968) 137.
[11] E.M. Serwicka, K. Bruckman, J. Haber, E.A. Paukshtis and E.N. Yurchenko, to be published.
[12] M.J.S. Dewar and W. Thiel, J. Am. Chem. Soc. 99 (1977) 4097 and 4899.
[13] H. Taketa, S. Katsuki, K. Eguchi, T. Seiyama and N. Yamazoe, J. Phys. Chem. 90 (1986) 2959.
[13] J.G. Highfield and J.B. Moffat, J. Catal. 95 (1985) 108.
[14] E. Broclawik, unpublished data.
[15] R.I. Maksimovskaya, M.A. Fedotov, V.A. Mastikhin, L.I. Kuznetsova and K.I. Matveev, Dokl. Akad. Nauk SSSR 240 (1978) 117.